CU

KEK Preprint 93-142
HUPD-9326
KOBE HEP-9310
KUNS-1225
OUHEP 93-5
OULNS 93-05
TMU-HEP 93-5
November 1993
H

Measurement of Open Charm Production in Two-Photon Processes with Detection of Electron-Inclusive Events

VENUS Collaboration

Submitted for publication

National Laboratory for High Energy Physics, 1993

KEK Reports are available from:

Technical Information & Library
National Laboratory for High Energy Physics
1-1 Oho, Tsukuba-shi
Ibaraki-ken, 305
JAPAN

Phone:	0298-64-1171	
Telex:	3652-534	(Domestic)
	(0)3652-534	(International)
Fax:	0298-64-4604	
Cable:	KEK OHO	
E-mail:	LIBRARY@JPNKEKVX	(Bitnet Address)
	library@kekvax.kek.jp	(Internet Address)

Measurement of Open Charm Production in Two-Photon Processes with Detection of Electron-Inclusive Events

VENUS Collaboration

S.Uehara[a], K.Abe[b], K.Amako[a], Y.Arai[a], T.Arima[c], Y.Asano[c], M.Chiba[d], Y.Chiba[e], M.Daigo[f], M.Fukawa[a], Y.Fukushima[a], J.Haba[g], H.Hanai[g], Y.Hemmi[h], M.Higuchi[i], F.Hinode[a], T.Hirose[d], Y.Homma[j], N.Hosoda[d] N.Ishihara[a], Y.Iwata[k], N.Kanda[g,1], N.Kanematsu[a,2], J.Kanzaki[a], R.Kikuchi[h], T.Kondo[a], T.T.Korhonen[a,ℓ], A.Krüger[g,3], H.Kurashige[h], J.MacNaughton[b,4], E.K.Matsuda[m], T.Matsui[a], M.Miura[c], K.Miyake[h], S.Mori[c], Y.Nagashima[g], Y.Nakagawa[n],T.Nakamura[o], I.Nakano[p], S.Odaka[a], K.Ogawa[a], T.Ohama[a], T.Ohsugi[k], H.Ohyama[k], A.Okamoto[h], A.Ono[q], T.Oyama[d], H.Sakamoto[h], M.Sakuda[a], M.Sato[i], N.Sato[a], M.Shioden[r], J.Shirai[a], M.Shirakata[c], T.Sumiyoshi[a], A.Suzuki[g,5], Y.Takada[c], H.Takaki[g,6], F.Takasaki[a], M.Takita[g], N.Tamura[m], K.Tobimatsu[s], T.Tsuboyama[a], Y.Unno[a], M.Utsumi[d,7], Y.Watase[a], F.Yabuki[d], Y.Yamada[a], T.Yamagata[n], Y.Yamamoto[g], Y.Yonezawa[t] and H.Yoshida[u]

[a] *KEK, National Laboratory for High Energy Physics, Tsukuba 305, Japan*
[b] *Department of Physics, Tohoku University, Sendai 980, Japan*
[c] *Institute of Applied Physics, University of Tsukuba, Tsukuba 305, Japan*
[d] *Department of Physics, Tokyo Metropolitan University, Hachioji 192-03, Japan*
[e] *Yasuda Women's Junior College, Hiroshima 731-01, Japan*
[f] *Wakayama Medical College, Wakayama 649-63, Japan*
[g] *Department of Physics, Osaka University, Toyonaka 560, Japan*
[h] *Department of Physics, Kyoto University, Kyoto 606, Japan*
[i] *Department of Applied Physics, Tohoku-Gakuin University, Tagajo 985, Japan*
[j] *School of Applied Medical Science, Kobe University, Kobe 654-01, Japan*
[k] *Department of Physics, Hiroshima University, Higashi-Hiroshima 724, Japan*
[ℓ] *Research Institute for High Energy Physics, Helsinki University, SF-00170, Helsinki, Finland*
[m] *Department of Physics, Okayama University, Okayama 700, Japan*
[n] *Division of Natural Sciences, International Christian University, Mitaka 181, Japan*
[o] *Faculty of Engineering, Miyazaki University, Miyazaki 889-01, Japan*
[p] *Institute of Physics, University of Tsukuba, Tsukuba 305, Japan*
[q] *Faculty of Cross-Cultural Studies, Kobe University, Kobe 657, Japan*
[r] *Department of Electronic and Computer Engineering, Ibaraki College of Technology, Katsuta 312, Japan*
[s] *Center for Information Science, Kogakuin University, Tokyo 163-91, Japan*
[t] *Tsukuba College of Technology, Tsukuba 305, Japan*
[u] *Naruto University of Education, Naruto 772, Japan*

[1] Present address: Institute for Cosmic Ray Research, University of Tokyo, Tanashi 188, Japan
[2] Present address: Department of Physics, University of California at Irvine, Irvine, CA92717, USA
[3] Present address: Carl Zeiss Japan, Tokyo 160, Japan
[4] Permanent address: Institute for High Energy Physics of Austrian Academy of Science, A-1050 Vienna, Austria
[5] Present address: Department of Physics, Kobe University, Kobe 657, Japan
[6] Present address: Synchrotron Radiation Laboratory, Institute for Solid State Physics, University of Tokyo, Tanashi 188, Japan
[7] Present address: Department of Applied Physics, Tokai University, Hiratsuka 259-12, Japan

Abstract

Experimental studies of open charm production in two-photon processes have been performed. In the measurement, charmed hadrons were identified by electrons from their semi-leptonic decays. The result was compared with calculations based on the direct process and photon-gluon fusion process by resolved photons. We found that the effect of the gluon component in a photon is substantial in the observed events.

1 Introduction

Charm production in two-photon processes, $\gamma\gamma \to c\bar{c}(+X)$, is a kind of high-$p_T$ phenomenon because a charm quark carries a significantly heavy mass compared with a typical mass scale for strong interactions. Therefore, a measurement of the process is very suitable for the study of the photon structure at a short distance, and is complimentary to measurements of the photon structure function made by high-Q^2 photons or multi-jet production processes.

By "no-tag" experiments at e^+e^- colliders, high-p_T hadron production is expected to show effects from resolved photons, where the photons are resolved into partons, *i.e.* quark, anti-quark or gluon[1]. Such a signature has been reported in measurements of multi-jet production[2]. However, the multi-jet production including light-quark production is quite complicated because it contains various types of origins. Several kinds of interactions regarding once- and twice-resolved photons (figs.1(b) and 1(c)) are expected to give a sizable contribution besides the direct process (fig.1(a)). Moreover, theoretical calculations for the processes include an artificial parameter p_T^{min}, which cuts the perturbative calculation at low-p_T region for elimination of double counting with the soft VDM calculation.

In the charm production, this condition is relaxed. The photon-gluon fusion process (the left diagram in fig.1(b)) only gives a sizable contribution among the resolved photon processes[3]. A large c.m. energy necessary to produce a charm quark pair keeps the cross section of the twice-resolved process small. The right diagram in fig.1(b) does not contribute to the charm production as a resolved photon process because a charm component in a photon is considered to be negligibly small before hard scattering[4]. This means that the contribution from the soft VDM process is also negligibly small, and the calculation does not require the ambiguous p_T^{min} parameter. Measurements of charm production give new independent information for the photon structure which is directly related to the gluon density in a photon#1.

Here, we report a measurement of the open charm production in two-photon processes in no-tag mode performed by an electron-inclusive method. All the previous measurements of the open charm production made at PEP[6], PETRA[7] and TRISTAN[8] used the D^* reconstruction method, in which D^* is identified by the decay mode $D^{*+} \to D^0\pi^+$ followed by $D^0 \to K^-\pi^+$, $K^-\pi^+\pi^0$, $K^-\pi^+\pi^-\pi^+$ and so on (and their charge-conjugate processes). A signature of excess over the expectation of the direct process is reported in these measurements, although their statistics are small. A new approach for this study has long been awaited.

2 Electron Inclusive Method and the VENUS Detector

We used the electron#2 inclusive method for identifying charmed hadrons. Almost all charmed hadrons can decay finally in semi-electronic modes directly or indirectly via one of $D^\pm$, D^0, $D_s^\pm$ and Λ_c. The average branching ratio for the semi-electronic decays is relatively large, about 10%. While, in the D^* reconstruction method, only $\approx$ 15% of the charm quark shows $D^{*+} \to D^0\pi^+$ decay[9]. A further reduction by a branching ratio of the D^0 decays in the process of D^0 identification results in less than 5% branching ratio for the charm identification. By the electron inclusive method, we can obtain a few times larger statistics than those by the D^* reconstruction method. A large background from hadron fakes can be rejected if a good capability of electron identification is invoked.

In the VENUS detector, a combination of the lead glass calorimeter[10] (LG) and the transition radiation detector[11] (TRD) gives an excellent electron identification at $p > 0.8$ GeV/c. With the electrons thus identified, we can detect charm quarks produced with lower transverse momenta more efficiently than those in the D^* reconstruction method because the maximum c.m. momentum for the semi-electronic decay is larger than 0.8 GeV/c.

The features of the VENUS detector are described elsewhere[12]. The Central Drift Chamber[13] (CDC) measures the momenta of charged particles in cooperation with a 0.75-T superconducting solenoid magnet. The momentum resolution is $\sigma_p/p = \sqrt{1.3^2 + (0.8p_T)^2}\%$ (p_T in GeV/c; we always measure transverse momentum p_T and polar angle θ with respect to the beam axis in this paper). Time of flights for charged particles are measured by the TOF counters[14] with a resolution of 250 ps. The energy deposit of electromagnetic shower is measured by the LG. The energy resolution for the LG is $\sigma_E/E \approx 8\%$ at 1 GeV. The TRD covers the angular acceptance $|\cos\theta| < 0.68$ which is fully overlapped with those of the CDC and the LG. Electromagnetic showers at small angles up to $|\cos\theta| = 0.99$ are measured by the Liquid Argon Calorimeters[15]. The Vertex Chamber(VTX)[16] is used here to estimate background electrons originating from neutral pions or photons. The quantity of material corresponds to 0.6% of a radiation length (X_0) between the collision point and the inner wall of the VTX and 8.7%X_0 between the collision point and the inner wall of the CDC in the direction perpendicular to the beam axis.

3 Event Selection

The data used in the present analysis were collected at c.m. energies from 57.6 to 59.7 GeV with an average $< \sqrt{s} >= 58.0$ GeV and correspond to an integrated luminosity of 162 pb^{-1}.

A trigger condition for selected events required at least two charged tracks with $p_T \geq 0.6$ GeV/c and $|\cos\theta| \leq 0.85$ and energy deposit $E_{\mathrm{LGseg}} \geq 0.64$ GeV in at least one LG segment. (The LG is divided into 58 segments.) We made the same E_{LGseg} cut in the software analysis. The trigger efficiencies for the tracks and for the LG segment were separately checked by real data, and each of them was confirmed to be greater than 95% at the threshold point mentioned above.

Events having visible energies of $E_{\mathrm{vis}} \leq 20$ GeV were selected. The number of charged tracks with $p_T \geq 0.2$ GeV/c and $|\cos\theta| \leq 0.89$ was required to be $N_{\mathrm{charged}} \geq 5$. The latter criterion was introduced to reduce backgrounds from lepton production, such as $(ee)\tau\tau$ and $(ee)ee\gamma$, and resonance production.

Among the above selected events, candidate electron tracks were searched in the momentum range $0.8 \leq p \leq 4.0$ GeV/c. The following fiducial and topological cuts were also applied: $|\cos\theta| \leq 0.68$ and $\eta_{\mathrm{iso}} \geq 10°$, where η_{iso} is an isolation angle between the candidate track and the nearest charged track. Tracks with $m_{\mathrm{TOF}} > 0.7$ GeV/c^2 and $p < 1.4$ GeV/c were rejected in order to eliminate protons and antiprotons with low momenta which gave larger energy deposit in the TRD than minimum-ionizing hadrons, where m_{TOF} is the mass derived from the TOF measurement. Electrons were identified by requiring appropriate energy deposit in the TRD and $E/p \geq 0.8$, where E/p is the quotient of the energy deposit in the LG to the momentum measured by the CDC. The energy cut for the TRD was set to give a momentum-independent efficiency for electrons. Fig.2 shows E/p distributions before and after the TRD cut. Finally, electrons originating from γ-conversion or π^0 Dalitz decay were eliminated by searching for another kissing track with $p_T \geq 70$ MeV/c near the electron candidates. After the selection, 149 events remained. Each candidate event was found to include only one electron candidate. The E/p distribution for the candidates is shown in fig.3.

4 Backgrounds

In the electron candidates, background from charged hadrons such as $\pi^\pm$ or $K^\pm$ remained. The number of the hadronic background events can be estimated in a reliable manner by making use of efficiencies of the TRD[17]. We can measure the detection efficiencies for electrons and hadrons by using experimental data because we have two independent electron-identifiers, the TRD and the LG. The efficiencies of the TRD were $\epsilon_{\mathrm{had}} = 3.5 \pm 0.4\%$ and $\epsilon_e = 66 \pm 3\%$, where ϵ_{had} and ϵ_e are the efficiencies for the applied cut for a hadron track and an electron track at the measured momentum region, respectively. We expect $33.1 \pm 5.4 \pm 4.4$ events for the background from charged hadrons (the first error is statistical and the second systematic). The estimated E/p distribution for the background is drawn in fig.3 by a dashed histogram.

The number of electrons originating from γ-conversion, Compton scattering or π^0 Dalitz decay is estimated by using the VTX, which is installed at the innermost part of the VENUS detector. Major part of such background electrons ($79 \pm 3\%$) originate at the outside of the VTX (Dalitz decay is a minor part) and do not leave trajectories in the VTX. We have measured the ratio of electron candidates without the VTX-trajectory although the VTX was not in operation for about 30% of the runs. It is estimated that the electron candidates include $41.7 \pm 3.8 \pm 4.1$ background events from π^0/γ origin.

In order to check the numbers of background events obtained by the above methods, we estimate them using Monte Carlo(MC) simulations for $e^+e^- \to e^+e^- +$ hadrons. We use only shapes of the distributions for observables such as E/p and momenta for final-state particles without relying on the absolute cross section for the MC events. The normalization for the number of the background events is made by adjusting the number of charged hadrons to the observation. The numbers of the background events by this method is estimated to be 31 ± 6 for the hadronic backgrounds and 40 ± 11 for those of π^0/γ origin, where the errors are systematic. The values are in good agreement with those obtained in the above estimation. We use the GVDM for light-quark production and the direct process for the charm production for generating the MC events. Since the fundamental observables such as E/p distribution and $\pi^0/\pi^\pm$ ratio are essential for the estimation, the results are hardly expected to be MC-model dependent.

Other backgrounds come from 1-γ annihilation (about 3 events, including those with initial state radiation of one or two photons), recoil electrons after emitting a high-Q^2 photon(about 1 event) and the decays of τ, K, J/ψ and b quark (about 1 event in total), which are estimated by Monte Carlo simulations. Summation of these backgrounds amounts to 5.8 ± 1.7 events.

The background events from the beam-gas collisions are negligibly small. This is confirmed by the distribution of original points of electron candidates along the beam direction, which shows a strong concentration around the collision point without tails. We note that the beam energy is too low to produce charm quarks efficiently on the residual gas nuclei.

5 Results and Expectations

The number of signal events is obtained by subtracting the estimated background events from the candidate events, to be $68.4 \pm 10.8 \pm 6.7$ events. The systematic error arises from ambiguities in the background estimation only. Systematic errors from other sources are counted in the calculations of the expected number of events described in the following.

The expected number of events has been calculated for the direct process and the photon-gluon fusion in the once-resolved photon process. The former is calculated by the program of Berends, Daverveldt and Kleiss[18], which includes all the relevant α^4 diagrams in the tree level. The charm quarks are fragmented into hadrons by the JETSET 7.3(Matrix-Element)[19]. The latter process is calculated by the program PYTHIA 5.6[19] with default parameters connected with the JETSET 7.3(Parton-Shower). The branching ratios for semi-electronic decays of D mesons in the LUND table have been updated according to the recent measurement[20].

The expected numbers of events are 29.4 ± 2.0 for the direct process and 10.0 ± 1.5, 45.5 ± 4.3 and 14.6 ± 1.8 for the photon-gluon fusion processes in which we used three sets of parameters for the gluon density according to DG[21], LAC1[22] and GRV[23], respectively. The contribution from twice-resolved processes is less than 0.7 event and neglected. The errors in the above values are the statistical ones in the Monte Carlo calculations. The systematic errors are $\pm 20 \pm 13\%$ for the direct process and $\pm 28 \pm 30\%$ for the photon-gluon fusion process. The first errors originate from ambiguities in the integrated luminosity (2.6%), detection efficiency(16% and 25% for the direct and photon-gluon fusion processes, respectively), the parton fragmentation(4%) and the decay branching ratio (11% and 12% for the direct and photon-gluon fusion processes, respectively). The second errors are from the theoretical calculations in the choices of the mass of charm quark and the assignment of energy scale Q^2 for the photon-gluon fusion#3.

6 Discussion

We make a comparison between the experimental results and the expectations in fig.4. The next-to-leading-order(NLO) QCD correction increases the direct process by 30%[3]. Such a correction for the photon-gluon fusion process is effectively taken into account in PYTHIA and Parton-Shower calculations originally with their default parameters. Therefore, we do not make any modification for the expectations calculated by PYTHIA.

The number of signal events is about twice the expectation from the direct process. The excess corresponds to the statistical significance higher than 2σ. However, the inclusion of the resolved photon process using DG, LAC1 or GRV parameters makes the calculation consistent with the experimental data.

We compare some distributions for the experimental data with those of the MC simulation which include both the direct process and the resolved photon process using LAC1 and GRV parameters(fig.5). The background distributions for the charged hadrons and electrons of the π^0/γ origin are subtracted from the experimental data on a bin-by-bin basis#4. The overall shapes of the distributions of visible invariant mass for the events W_{vis}, and p_T for the electron candidates are consistent with the calculations#5. The experimental data includes significantly more low-thrust events than expected by the direct process. In the angular energy flow distribution measured by the electromagnetic calorimeters, there is an enhancement at small angles which is not reproduced by the direct process and is considered to come from the remnants of the resolved photons. These facts indicate that a substantial part of the experimental data comes from the photon-gluon fusion process. The expectation from "direct+LAC1" shows qualitative agreement for all the distributions, while "direct+GRV", and "direct+DG" whose contribution is slightly smaller than that of "direct+GRV", seem to be still insufficient to explain the features in the last two distibutions.

It must be noted, however, that LAC1 is not justified by the present analysis only, since the gluon density function $G(x)$ has large ambiguity in its shape as well as in its size. $G(x)$ must be determined experimentally by investigating distributions in various channels.

7 Conclusion

The process $\gamma\gamma \rightarrow c\bar{c}(+X)$ gives new information for the photon structure which is directly related to the gluon density. We measured the process by the electron inclusive method for the first time. An excess over the direct process was observed in the number of signal events at a significant level. The result was compared with the theoretical calculations including the resolved photon processes. The observed thrust and angular energy-flow distributions corroborate that the excess comes from the photon-gluon fusion process by a gluon component in a photon.

Acknowledgement

The authors gratefully acknowledge the outstanding efforts of the TRISTAN accelerator group for excellent machine operation. They are indebted to the KEK support groups of cryogenics and computation. Thanks also go to the technical staffs of the collaborating institutes, who enabled us to take data continuously. They also thank Dr. K.Hagiwara and Dr. M.Drees for their valuable advice concerning the theoretical calculations.

#1 This situation is similar to that in charm photoproduction on nucleus, $\gamma A \rightarrow c\bar{c}+X$. It is reported that this process can be well explained by the photon-gluon fusion process and is useful to extract the gluon density in a nucleon[5].

#2 "Electron" is a generic name for e^- and e^+ in this paper.

#3 The errors correspond to variations of the mass of charm quark with 0.2 GeV/c^2 from the chosen values (1.60 and 1.35 GeV/c^2 for the direct process and for the photon-gluon fusion process, respectively) and the assignment of Q^2, which is varied from $(m_{T1}^2 + m_{T2}^2)/2$ to $W_{\gamma g}^2$, where m_{Ti} is the transverse mass of each charm quark, and $W_{\gamma g}$ the c.m. energy for the photon-gluon system.

#4 We assume that the charged hadron background has the same shapes in the distributions as those events which satisfy the selection criteria for the present analysis without including the requirement for the TRD and have sufficiently small energy deposit in the TRD to guarantee the electron candidate being a charged hadron. We also assume that the background originated from π^0/γ has the same shapes as the candidate events in which electron candidates have no VTX-trajectory. The enhancements in low thrust and forward energy-flow in figs.5(c) and 5(d), respectively, are confirmed also in low-background events, which are selected by tighter cuts in the TOF and impact parameter for the electron candidates.

#5 We define here W_{vis} as $\sqrt{E_{\text{vis}}^2 - (\sum p_{z\text{vis}})^2}$ by assuming p_T-balance in the final state, where the z-axis is defined as the e^- beam direction. We also calculate the thrust in the p_z-balanced frame after boosting the observed final-state particles in the z direction.

References

[1] M.Drees and R.M.Godbole, Nucl. Phys. **B339** (1990) 355; M.Drees and R.M.Godbole, preprint BU-TH-92/5 (1992).

[2] AMY Collaboration, R.Tanaka *et al.*, Phys. Lett. **B277** (1992) 215; ALEPH Collaboration, D.Buskulic *et al.*, Phys. Lett. **B313** (1993) 509; TOPAZ Collaboration, H.Hayashii *et al.*, Phys. Lett. **B314** (1993) 149.

[3] M.Drees, M.Krämer, J.Zunft and P.M.Zerwas, Phys. Lett. **B306** (1993) 371.

[4] B.Margolis, Phys. Rev. **D17** (1978) 1310.

[5] Tagged Photon Spectrometer Collaboration, J.C.Anjos *et al.*, Phys. Rev. Lett. **65** (1990) 2503.

[6] TPC/2γ Collaboration, M.Alston-Garnjost *et al.*, Phys. Lett. **B252** (1990) 499.

[7] JADE Collaboration, W.Bartel *et al.*, Phys. Lett. **B184** (1987) 288; TASSO Collaboration, W.Braunschweig *et al.*, Z. Phys. **C47** (1990) 499.

[8] TOPAZ Collaboration, R.Enomoto *et al.*, KEK preprint 93-107 (1993).

[9] VENUS Collaboration, F.Hinode *et al.*, Phys. Lett. **B313** (1993) 245.

[10] T.Sumiyoshi *et al.*, Nucl. Instrum. Meth. **A271** (1988) 432.

[11] N.Terunuma *et al.*, Nucl. Instrum. Meth. **A323** (1992) 471.

[12] VENUS Collaboration, K.Abe *et al.*, J. Phys. Soc. Jpn., **561** (1987) 3763.

[13] R.Arai *et al.*, Nucl. Instr. and Meth. **A217** (1983) 181.

[14] Y.Hemmi *et al.*, Jpn. J. Appl. Phys. **26** (1987) 982.

[15] Y.Fukushima *et al.*, IEEE Trans. Nucl. Sci. **36** (1989) 670.

[16] Y.Yamada *et al.*, Nucl. Instrum. Meth. **A330** (1993) 64.

[17] VENUS Collaboration, K.Abe *et al.*, Phys. Lett. **B313** (1993) 288.

[18] F.A.Berends, P.H.Daverveldt and R.Kleiss, Nucl. Phys. **B253** (1985) 441 and Comp. Phys. Comm. **40** (1986) 285.

[19] T.Sjöstrand, preprint CERN-TH.6488/92 (1992).

[20] Mark-III Collaboration, Z.Bai *et al.*, Phys. Rev. Lett. **66** (1991) 1011.

[21] M.Drees and K.Grassie, Z. Phys. **C28** (1985) 451.

[22] H.Abramowicz, K.Charchula and A.Levy, Phys. Lett. **B269** (1991) 458.

[23] M.Glück, E.Reya and A.Vogt, Phys. Rev. **D46** (1992) 1973.

Figure Captions

Fig.1: Feynman diagrams for the direct process(a), once-resolved processes(b) and twice-resolved processes(c). Each solid line in the right diagram in (c) can be a quark or an anti-quark to conserve the quark-number. There are other diagrams not drawn in (c).

Fig.2: E/p distributions for the tracks before(dashed line) and after the TRD cut(solid line).

Fig.3: E/p distribution for the candidate tracks(dot points with error bars). The dashed histogram is estimated hadronic backgrounds.

Fig.4: Comparison of the numbers of observed signal events and the expectations. The error bar for the "observed" is statistical only. The region represented by arrows corresponds to the error for the expectation value, where the statistical and systematic errors are quadratically summed.

Fig.5: Various distributions for the experimental data (dot points with error bars) after subtracting the backgrounds from charged hadrons and π^0/γ origin and for the calculations from the direct process(solid histograms), "direct + LAC1" (dashed histograms) and "direct + GRV" (dotted histograms). The experimental data includes about 5.8-event backgrounds from the other sources (see the text in section 4). No NLO QCD corrections are applied for the direct process. The distributions are for W_{vis}(a), p_T for the electron candidate(b), the thrust in the p_z-balanced frame of observed final-state particles(c) and angular energy-flow distribution in electromagnetic calorimeters summed over the events(d). There is no entry in (b) for $p_T(e) > 3$ GeV/c.

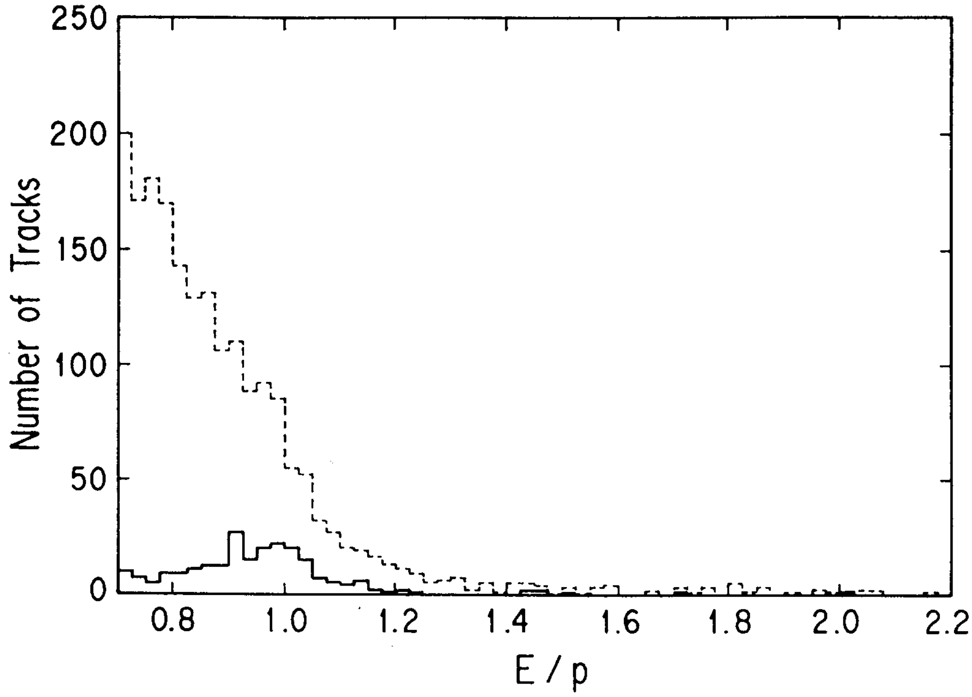

Number of Tracks
250
200
150
100
50
0
0.8
1.0
1.2
1.4
1.6
1.8
2.0
2.2
E / p

Fig.2

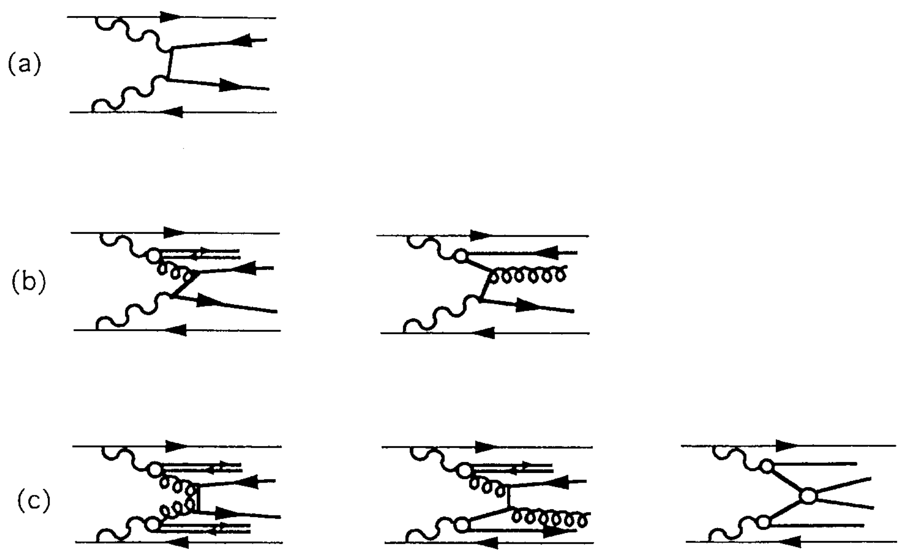

(a)
(b)
(c)

Fig.1

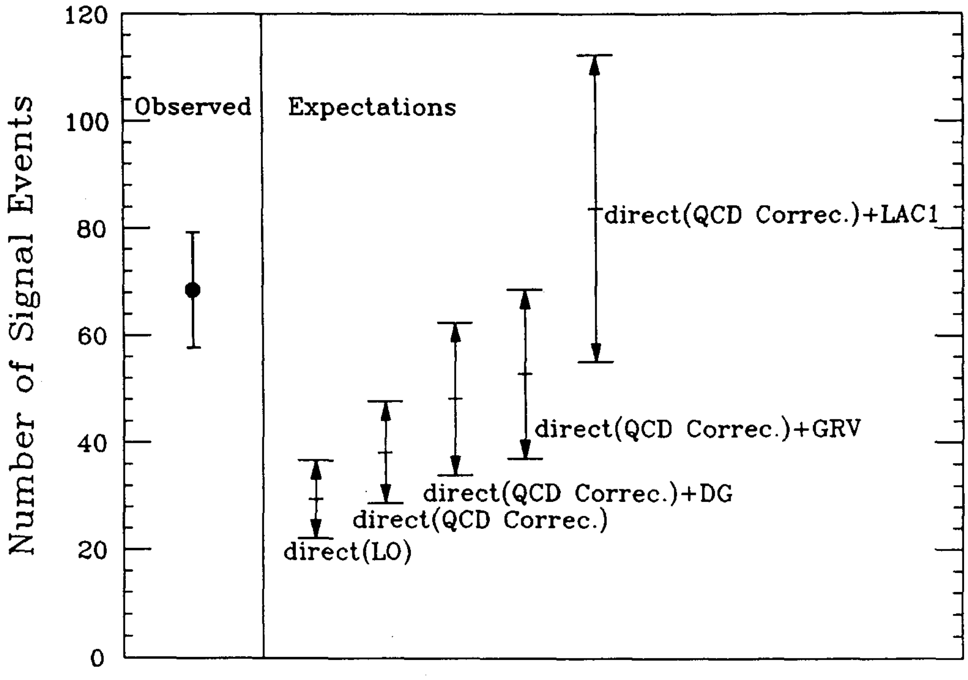
Number of Signal Events
120
100
80
60
40
20
0
Observed
Expectations
direct(QCD Correc.)+LAC1
direct(QCD Correc.)+GRV
direct(QCD Correc.)+DG
direct(QCD Correc.)
direct(LO)

Fig.4

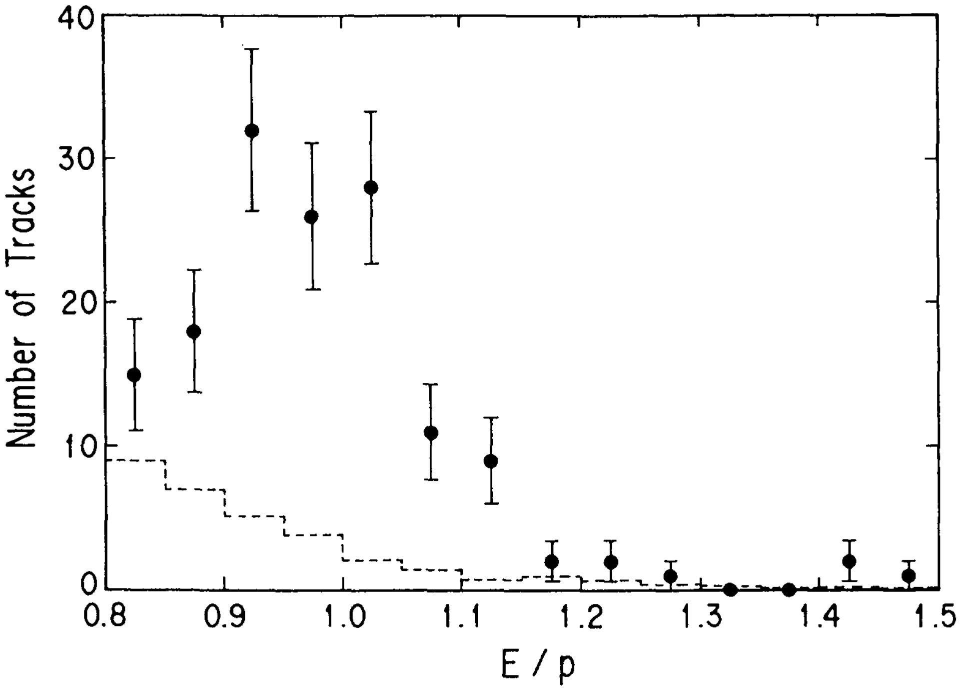
Number of Tracks
40
30
20
10
0
0.8
0.9
1.0
1.1
1.2
1.3
1.4
1.5
E / p

Fig.3

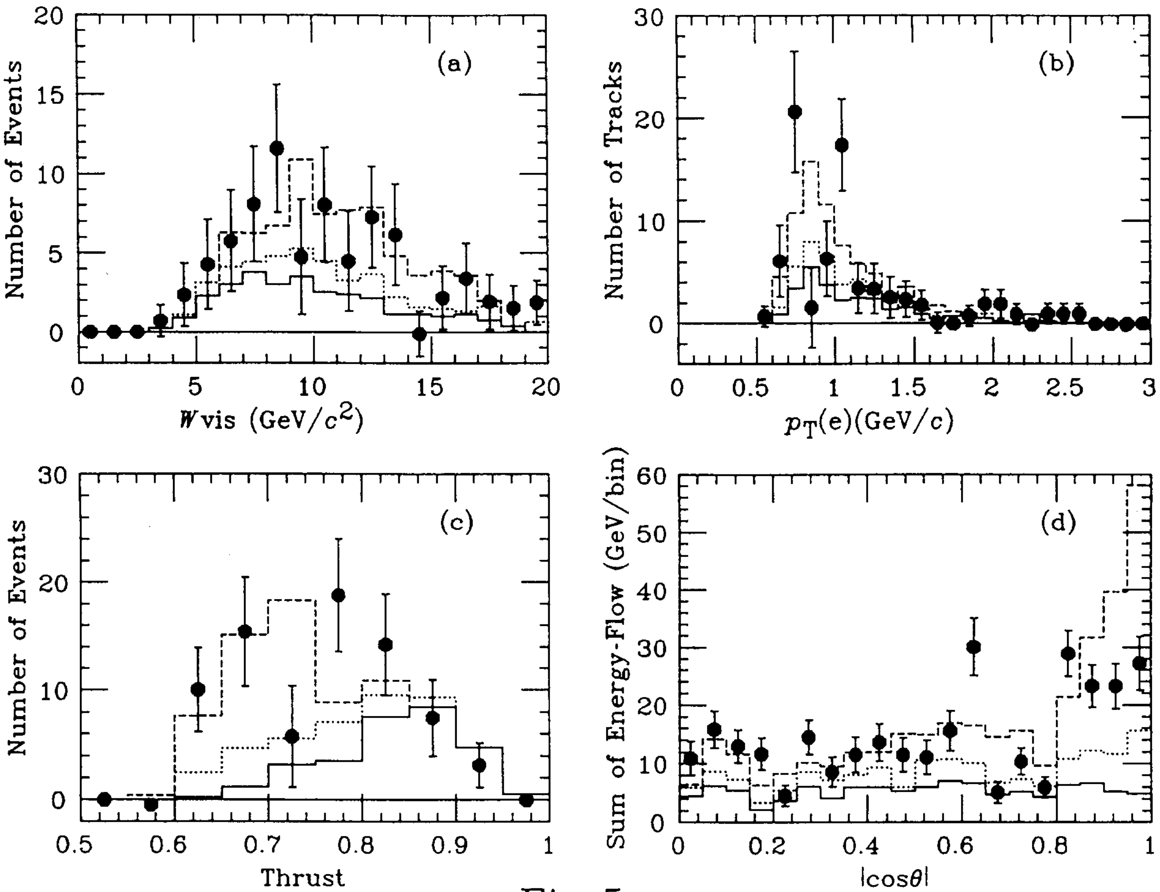
(a)
(b)
(c)
(d)
Number of Events
Number of Tracks
Number of Events
Sum of Energy-Flow (GeV/bin)
Wvis (GeV/c2)
pT(e)(GeV/c)
Thrust
|cosθ|

Fig.5